Coherent elastic energy calculation of ω particles in β matrix for Zr–Nb alloys

Bin Tang · Hong-Chao Kou · Hui Chang · Jin-Shan Li · Lian Zhou

Abstract The misfit and coherent elastic energy caused by ω particles in β matrix is quantitatively calculated in this study. First, the coherent strain matrixes for four ω variants are established including the misfit parameters based on Khachaturyan's theory. Then, the misfit and coherent elastic energy in athermal $\beta \rightarrow \omega$ transition, and isothermal $\beta \rightarrow \omega$ transition are calculated, respectively. The calculation results indicate that the coherent elastic energy gets maximum value when $x_{Nb} = 0.08$ (Nb content) and gets minimum value when $x_{Nb} = 0.1518$ in quenching Zr–Nb alloys, which are in fair agreement with experimental results. For isothermal $\beta \rightarrow \omega$ transition, the misfit and coherent elastic energy depend on composition and aging temperature. The misfit caused by isothermal ω phase is much larger than the one caused by athermal ω phase. This results in larger coherent elastic energy in isothermal $\beta \rightarrow \omega$ transition. In addition, the misfit is found as an approximate linear function of temperature and composition for Zr–Nb alloys, and the coherent elastic energy is revealed as an increasing function of $|v_F - v_S|$ for the two kinds of transition.

Introduction

The investigation of metastable ω phase in Zr- and Ti-based alloys is a subject of intense interest and activity, which has been undertaken for more than fifty years. Metastable ω phase not only has the marked effect on the mechanical and physical 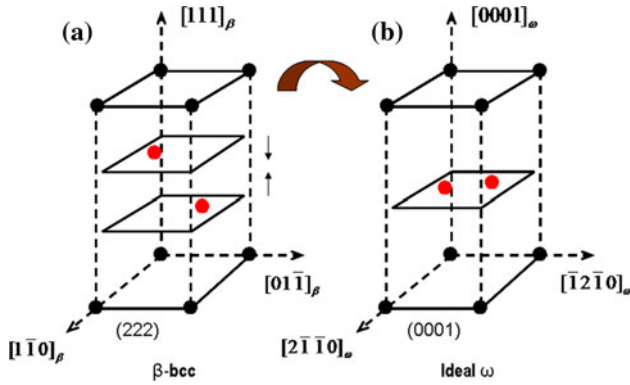properties of materials directly, but also can affect mechanical properties indirectly by playing a substantial role in α nucleation, which has hotly been studied in recent years [1–3]. Two kinds of ω phase, athermal ω phase and isothermal ω phase, produced by quenching from single β phase field and aging at low temperature respectively, have been mainly investigated in engineering materials during heat-treatment process. The ordinary morphology of athermal ω particles is ellipsoidal, the size being about 5 nm in diameter. However, the morphology of isothermal ω particles exhibits ellipsoidal (such as Zr–Nb) or cuboidal (such as Ti–Fe) determined by lattice misfit, while the normal size is between 20 and 50 nm [4].

The transition mechanism of β phase with bcc structure transforming to ω phase with hexagonal structure is thought to be caused by (111) planes collapsing [4]. As shown in Fig. 1, a pair of $(222)_\beta$ planes collapses to the intermediate position, and then, the ideal ω phase with sixfold rotation symmetry is produced. Once the collapse is incomplete, the trigonal structure ω phase is created. Based on the lattice correspondence shown in Fig. 1, the lattice parameters of ω phase can be expressed as $a_\omega = \sqrt{2}a_\beta$, $\left(c_\omega = \sqrt{3}/2\right)a_\beta$.

The ω phase precipitated in Zr- and Ti-based alloys has been investigated deeply and widely discussed. However, some important issues about ω phase and $\beta \rightarrow \omega$ transition have not been revealed, for example, why the athermal ω morphology so developed is ellipsoidal, rather than a plate-like martensite? Which kind of energy determines the ω morphology, elastic energy, or interfacial energy? Why the misfit between isothermal ω phase and β-phase can change the ω morphology (from ellipsoidal to cuboidal)?

The coherency strain between ω particle and β matrix is very important when answering these questions. Cook calculated the elastic energy modulus of Zr–Nb alloys in h-space first by means of defect force field theory [6].

B. Tang (✉) · H.-C. Kou · H. Chang · J.-S. Li · L. Zhou
State key Laboratory of Solidification Processing,
Northwestern Polytechnical University, Xi'an 710072, China
e-mail: toby198489@163.com

Fig. 1 Schemes of $\beta \rightarrow \omega$ transition, representing the collapse of the (111) planes of the bcc structure; **a** the ABCABC... sequences of atomic plane arrangements in β-lattice. **b** The planar arrangement of $(0001)\omega$ atomic planes in the ideal ω-lattice [5]

Recently, on the basis of droplet model, Susan et al. calculated the reciprocal elastic energy modulus when they studied heterophasic fluctuations of incommensurate ω phase in Cu–Zn system [7].

The misfit and coherent strain energy of ω phase in the β matrix are our primary concerns in this study. In order to evaluate the effect of coherent elastic energy on growing process of ω phase, we characterized the misfit by lattice parameters (a_β, a_ω, and c_ω) and then calculated the coherent strain energy phenomenologically and quantitatively based on Khachaturyan's theory in this article. In the calculation model, two misfit parameters (v_F and v_S) and four strain matrixes (corresponding to four variants) are included.

Calculation model

Analytical expression of coherent elastic energy

As has been widely investigated, the athermal $\beta \rightarrow \omega$ transition only involves the "shuffle" process, and it is a coherent phase transformation without volume change. The strain energy function that is associated with phase transformation in the stress-free state has been suggested by Khachaturyan [8]. In Ref. [8], the stress-free strain tensors $\varepsilon_{ij}^0(p)$ have been introduced, and the total elastic strain energy counted from the stress-free state can be presented as

$$E_{\text{elast}} = \Delta E_0 + \Delta E_{\text{relax}} = \Delta E_0 + E_{\text{relax}}^{\text{hom}} + E_{\text{relax}}^{\text{heter}} \tag{1}$$

where

$$\Delta E_0 = \frac{1}{2}\sum_P V_P \lambda_{ijkl}\varepsilon_{ij}^o(p)\varepsilon_{kl}^o(p) \tag{2}$$

$$E_{\text{relax}}^{\text{hom}} = -\frac{V}{2}\sum_{p=1}^{v}\sum_{q=1}^{v}\lambda_{ijkl}\varepsilon_{ij}^o(p)\varepsilon_{kl}^o(q)w_p w_q \tag{3}$$

$$E_{\text{relax}}^{\text{heter}} = -\frac{1}{2}\sum_{p,q}\int\frac{d^3k}{(2\pi)^3}(k\hat{\sigma}^o(p)\hat{G}(k)\hat{\sigma}^o(q)k)\tilde{\theta}_p(k)\tilde{\theta}_q^*(k) \tag{4}$$

In Eqs. 1–4, ΔE_0 is the energy required to elastically "squeeze" all the stress-free orientation variants of the ω phase back into their parent phase; $E_{\text{relax}}^{\text{hom}}$ and $E_{\text{relax}}^{\text{heter}}$ are the energy reductions due to the macroscopic homogeneous strain relaxation and local heterogeneous strain, respectively [9]. $V_p = \int \theta_p(r)dV$ is the total volume of p-th kind phases, and $w_p = V_p/V$ is the volume fraction of p-th orientation. $G_{ij}(k)$ is the inverse tensor to $(\hat{G}^{-1})_{ij} = \lambda_{iklj}k_k k_l$. $\tilde{\theta}_p(k)$ is the Fourier transform of the shape function $\theta_p(r)$, which is equal to unity inside an orientation, and to zero outside it.

Coherent strain matrix

The stress-free strain $\varepsilon_{ij}^0(p)$ for athermal $\beta \rightarrow \omega$ transition can be obtained by assuming that the total elastic energy is the sum of homogeneous isotropic strain in the $\{111\}_{\text{bcc}}$ planes and the strain along the $\langle111\rangle_{\text{bcc}}$ directions. The similar analysis method has been used by Khachaturyan [8] to treat the strain caused by atom shuffling during transformation process.

According to crystal lattice correspondence, the relationship between lattice parameters of ω structure and β structure is given by

$$\sqrt{2}\cdot a_\beta \rightarrow a_\omega, \sqrt{3}\cdot a_\beta \rightarrow 2c_\omega \tag{5}$$

The strain in the $(111)_\beta$ is isotropic:

$$\varepsilon_1 = \frac{a_\omega - \sqrt{2}\cdot a_\beta}{\sqrt{2}\cdot a_\beta} = \frac{a_\omega}{\sqrt{2}\cdot a_\beta} - 1 \tag{6}$$

Then, the invariant form of an isotropic strain in the $(111)_\beta$ plane can be written as

$$\varepsilon_{ij}^{(1)} = \varepsilon_1(\delta_{ij} - e_i^{[111]}\cdot e_j^{[111]}) \tag{7}$$

where $e^{[111]}$ is the unit vector normal to a $(111)_\beta$ plane. The strain value along the $[111]_\beta$ direction normal to the $(111)_\beta$ planes is given by

$$\varepsilon_2 = \frac{2c_\omega - \sqrt{3}\cdot a_\beta}{\sqrt{3}\cdot a_\beta} = \frac{2c_\omega}{\sqrt{3}\cdot a_\beta} - 1 \tag{8}$$

The invariant form of this strain is

$$\varepsilon_{ij}^{(2)} = \varepsilon_2 e_i^{[111]}\cdot e_j^{[111]} \tag{9}$$

From Eqs. 7 and 9, the total strain is

$$\varepsilon_{ij}(1) = \varepsilon_{ij}^{(1)} + \varepsilon_{ij}^{(2)} = \varepsilon_1(\delta_{ij} - e_i^{[111]} \cdot e_j^{[111]}) + \varepsilon_2 e_i^{[111]} \cdot e_j^{[111]}$$

$$= \varepsilon_1 \delta_{ij} + (\varepsilon_2 - \varepsilon_1) e_i^{[111]} \cdot e_j^{[111]}$$

$$= \left(\frac{a_\omega}{\sqrt{2} \cdot a_\beta} - 1 \right) \delta_{ij} + \left(\frac{2c_\omega}{\sqrt{3} \cdot a_\beta} - \frac{a_\omega}{\sqrt{2} \cdot a_\beta} \right)$$

$$\cdot e_i^{[111]} \cdot e_j^{[111]} \tag{10}$$

where $e^{[111]} = (1/\sqrt{3}, 1/\sqrt{3}, 1/\sqrt{3})_\beta$

We assume $v_s = \frac{a_\omega}{\sqrt{2} \cdot a_\beta} - 1$, and $v_F = \frac{2c_\omega}{\sqrt{3} \cdot a_\beta} - \frac{a_\omega}{\sqrt{2} \cdot a_\beta}$; v_S and v_F are associated to lattice mismatch between β structure and ω structure, respectively. Then Eq. 10 can transform to

$$\varepsilon_{ij}(1) = \begin{pmatrix} v_s + \frac{1}{3}v_F, \frac{1}{3}v_F, \frac{1}{3}v_F \\ \frac{1}{3}v_F, v_s + \frac{1}{3}v_F, \frac{1}{3}v_F \\ \frac{1}{3}v_F, \frac{1}{3}v_F, v_s + \frac{1}{3}v_F \end{pmatrix} \tag{11a}$$

Using the same method, $\varepsilon_{ij}(2)$, $\varepsilon_{ij}(3)$, and $\varepsilon_{ij}(4)$ can be obtained:

$$\varepsilon_{ij}(2) = \begin{pmatrix} v_s + \frac{1}{3}v_F, -\frac{1}{3}v_F, -\frac{1}{3}v_F \\ -\frac{1}{3}v_F, v_s + \frac{1}{3}v_F, \frac{1}{3}v_F \\ -\frac{1}{3}v_F, \frac{1}{3}v_F, v_s + \frac{1}{3}v_F \end{pmatrix} \tag{11b}$$

$$\varepsilon_{ij}(3) = \begin{pmatrix} v_s + \frac{1}{3}v_F, -\frac{1}{3}v_F, \frac{1}{3}v_F \\ -\frac{1}{3}v_F, v_s + \frac{1}{3}v_F, -\frac{1}{3}v_F \\ \frac{1}{3}v_F, -\frac{1}{3}v_F, v_s + \frac{1}{3}v_F \end{pmatrix} \tag{11c}$$

$$\varepsilon_{ij}(4) = \begin{pmatrix} v_s + \frac{1}{3}v_F, \frac{1}{3}v_F, -\frac{1}{3}v_F \\ \frac{1}{3}v_F, v_s + \frac{1}{3}v_F, -\frac{1}{3}v_F \\ -\frac{1}{3}v_F, -\frac{1}{3}v_F, v_s + \frac{1}{3}v_F \end{pmatrix} \tag{11d}$$

As a consequence, the stress–free strain can be expressed by Eq. 11 corresponding to the four variants, while they are determined by the crystal lattice mismatch between β and ω.

Results and discussion

Database of lattice parameters for Zr–Nb alloys

The structure properties of ω phase and β phase in Zr–Nb alloys have been investigated systematically by Aurelio et al [10–13]. Based on their research studies, an extensive database with the lattice parameters of metastable phases

(α, ω, β) in Zr–Nb alloys has been developed by direct experiments (high-quality neutron-diffraction measurements and Rietveld analysis) and "reference behavior".

The available lattice parameters vs. at.% Nb ($0 < x_{Nb} < 1$) content for athermal ω and β introduced by quenching can be described by expressions [10].

$$a_\beta(x_{Nb})[nm] = 0.35878(7) - 0.0288(3)x_{Nb} \tag{12}$$

$$a_\omega(x_{Nb})[nm] = 0.50380(1) - 0.0202(2)x_{Nb} \tag{13}$$

$$c_\omega(x_{Nb})[nm] = 0.31360(1) - 0.0467(2)x_{Nb} \tag{14}$$

The evolution of the lattice parameters vs. Nb content and temperature of the ω and β phases upon aging are shown as follows [10]:

$$a_\beta(x_{Nb}, T)[nm] = (0.35878(7) - 0.0288(3)x_{Nb})$$
$$\times \exp[6.8(5) \times 10^{-6}(T - T_R) + 1.0(2) \times 10^{-9}(T^2 - T_R^2)] \tag{15}$$

$$a_\omega(x_{Nb}, T)[nm] = (0.5038(1) - 0.0202(2)x_{Nb})$$
$$\times \exp[7.9(4) \times 10^{-6}(T - T_R)] \tag{16}$$

$$c_\omega(x_{Nb}, T)[nm] = (0.3136(1) - 0.0467(2)x_{Nb})$$
$$\times \exp[3.5(3) \times 10^{-6}(T - T_R)] \tag{17}$$

In Ref. [14], the elastic constants of Zr–Nb alloys were treated as a linear function of composition by Yoshiaki Toda et al.

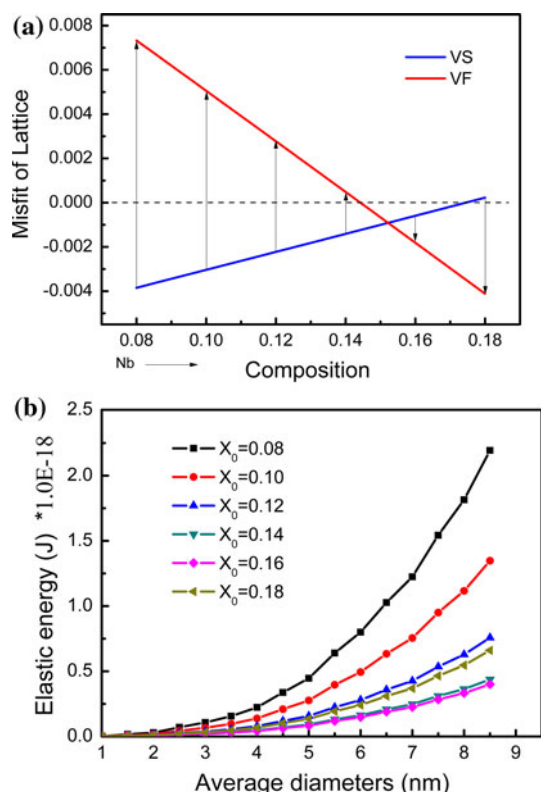$$C_{11} = (-1.14 \cdot (1 - x_{Nb}) + 2.07) \times 10^{11} \, N \, m^{-2} \tag{18a}$$

$$C_{12} = (-0.591 \cdot (1 - x_{Nb}) + 1.34) \times 10^{11} \, N \, m^{-2} \tag{18b}$$

$$C_{44} = (0.581 \cdot (1 - x_{Nb}) + 2.89) \times 10^{10} \, N \, m^{-2} \tag{18c}$$

The calculation of coherent elastic energy in athermal $\beta \rightarrow \omega$ transition

On the basis of lattice parameters database and elastic constants expressions (Eqs.12–14, 18), the coherent strain energy produced in athermal $\beta \rightarrow \omega$ transition is calculated quantitatively in this section. For athermal $\beta \rightarrow \omega$ transition, the misfit between athermal ω phase and β matrix is mainly determined by Nb content. Figure 2a illustrates the variety of misfit (represented by v_S and v_F) vs. Nb content. As shown in Fig. 2a, the misfit of lattice has an approximate linear relationship with composition. The $|v_F - v_S|$ obtains maximum and minimum values, at $x_{Nb} = 0.08$ and at $x_{Nb} = 0.1518$, respectively.

To simplify the calculation, the morphology of ω particles was set as sphere in the model. The coherent strain energy is calculated in 25 nm³ system with the size of athermal ω particle being about 5 nm as usual. We set eight particles for four variants in the calculation space, and the particles are separated from one another. As expressed in Eq. 4, the coherent elastic energy is
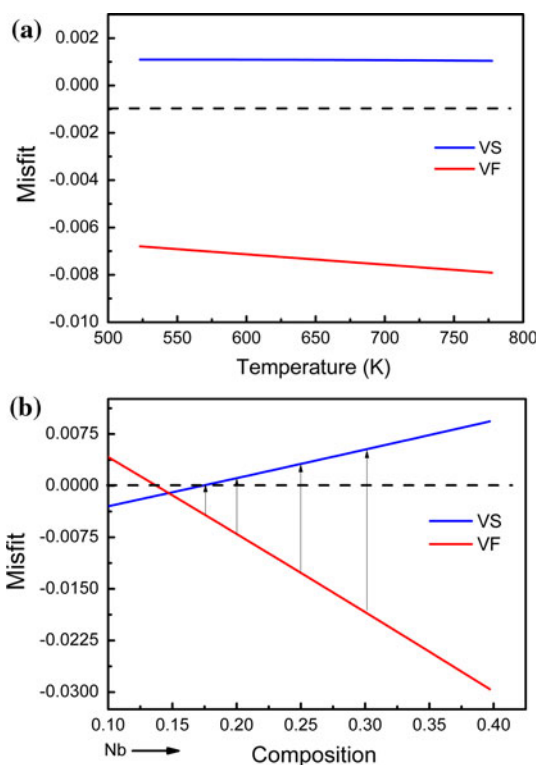
Fig. 2 a The lattice misfit changes associated with the Nb content which is expressed by Eqs. 12–14. **b** The calculation results of coherent strain energy for different Nb contents

Fig. 3 a Relationship between misfit and temperature when $x_{Nb} = 0.2$. **b** Relationship between misfit and composition when $T = 573$ K

determined by the composition and particle size. For a particular composition, the coherent strain energy has a strict form as a linear function of the particle volume ($E_{co} = K r^3$). The calculation results are shown in Fig. 2b. In the composition range, $0.08 \leq x_{Nb} \leq 0.18$, the maximum coherent strain energy appears at $x_{Nb} = 0.08$, and the minimum coherent strain energy appears at $x_{Nb} = 0.1518$. When $x_{Nb} < 0.1518$, the coherent elastic energy deceases with increasing Nb content; when $x_{Nb} > 0.1518$, the energy increases with increasing Nb content. These results have been confirmed by Grad and Aurelio [12, 15] who found that the atoms of ω phase displaced slightly when Nb content is as high as 0.15, which represents small misfit. On the other hand, Sass and Borie noted that the athermal ω phase had the ideal structure in Zr–8%Nb alloy [16], which represents complete collapse and larger misfit. Furthermore, the coherent strain energy has corresponding relationship with $|v_F–v_S|$ as found from comparing Fig. 2a and b.

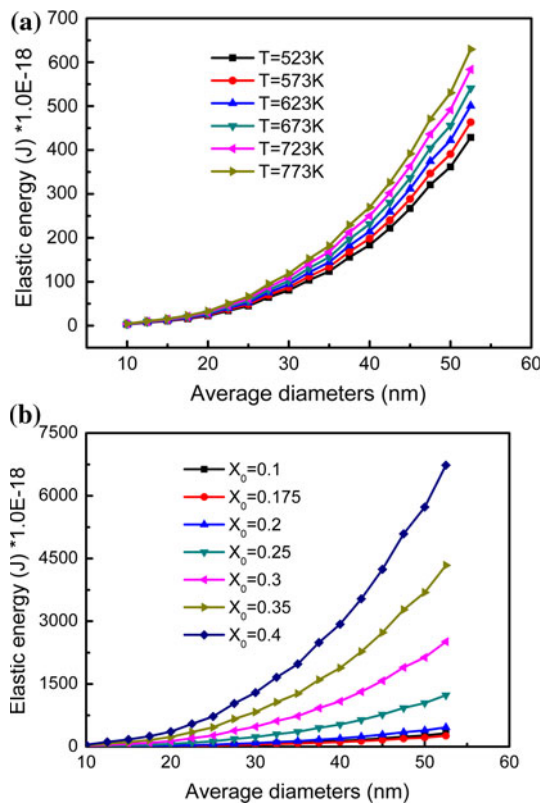The calculation of coherent elastic energy in isothermal $\beta \rightarrow \omega$ transition

Depending on Aurelio's work for aging Zr–Nb alloys, we can acquire the variety of misfit with aging temperature and composition. The changes in misfit associated with temperature and composition are shown in Fig. 3. It is apparent from Fig. 3 that v_S and v_F have approximate linear relationship with aging temperature and composition. In addition, v_F is nearly seven times larger than v_S. The $|v_F–v_S|$ obtains minimum value at $x_{Nb} = 0.147$. From the results thus obtained, it is clear that the misfit produced by isothermal ω precipitation is larger than that caused by athermal ω particles, and it is especially more obvious for high Nb content alloys. The difference maybe caused by the reconstruction of lattice during aging process.

The coherent strain energy is calculated in 125 nm³ system as the isothermal ω particle is much bigger than athermal ω particle. We set eight separately spherical particles for four variants in the calculation space as well. The coherent strain energies produced by isothermal ω precipitation for different temperatures and compositions are shown in Fig. 4. The energy increases with rising temperature (Fig. 4a). In Fig. 4b, the coherent elastic energy exhibits first a decreased, and then an increased regulation as well with increasing Nb content, and reaches minimum at $x_{Nb} = 0.147$. Figures 3 and 4 demonstrate that the coherent strain energy caused by isothermal ω phase is also mainly determined by $|v_F–v_S|$, although the role played by v_S is much smaller than that of v_F. Owing to the increase
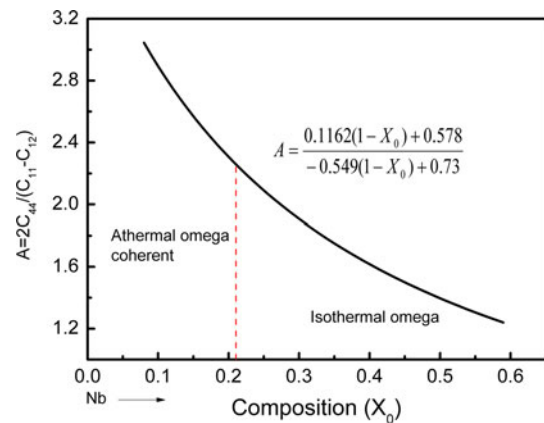
Fig. 4 a The coherent strain energy at different temperatures when $x_{Nb} = 0.2$. **b** The coherent strain energy at different compositions when $T = 573$ K

Fig. 5 The elastic anisotropy factor A of Zr–Nb alloys at various compositions

Therefore, the athermal ω phase tends to present ellipsoids morphology. For isothermal ω phase, different alloy systems have different morphologies depending on lattice misfit. In small misfit systems (such as: Zr–Nb, Ti–Nb) the morphologies of ω particles exhibit ellipsoidal, while a larger misfit (such as: Ti–V, Ti–Fe) will lead to cuboidal-like morphologies [19].

in misfit, the coherent elastic energy produced in isothermal $\beta \rightarrow \omega$ transition is much larger.

Anisotropy of elastic energy

In a cubic system, the elastic interaction energy depends on Zener's anisotropy factor, $A = 2C_{44}/(C_{11} - C_{12})$ [17, 18]. "$A = 1$" represents elastic isotropic condition. According to Eq. 18, the elastic anisotropy factor (A) for Zr–Nb alloys is depicted as a function of composition (Fig. 5). The elastic anisotropy factor of Zr–Nb alloys decreases with increasing Nb content and the factor $A > 1$ in the available composition range. Therefore, the $\langle 100 \rangle$ directions are elastically the softest, and the $\langle 111 \rangle$ directions are elastically the hardest [17]. The particle morphology is related to the elastic energy and surface energy [19]. If the elastic energy plays dominant role in $\beta \rightarrow \omega$ transition, then the precipitates in cubic matrix tend to be quadrate. If the surface energy is greater, then the particle shape is determined by the minimization of surface energy which is anisotropic. It is clear from the calculation results that the coherent strain energy produced by athermal ω phase is much smaller than that created by isothermal ω phase.

Conclusions

In this study, the coherent elastic energies of Zr–Nb alloys during athermal $\beta \rightarrow \omega$ transition and isothermal $\beta \rightarrow \omega$ transition were, respectively, calculated based on the coherent strain matrixes and the definition of misfit. For athermal $\beta \rightarrow \omega$ transition, the misfit of lattice has approximately a linear relationship with composition. The coherent elastic energy first decreases and then increases with rising Nb content. The maximum and minimum values appear at $x_{Nb} = 0.08$ and $x_{Nb} = 0.1518$, respectively. For isothermal $\beta \rightarrow \omega$ transition, the misfit is related to aging temperature and composition. The coherent elastic energy monotone increases with rising temperature, while it exhibits first decreased and then increased regulation as well with increasing Nb content, and reaches minimum at $x_{Nb} = 0.147$. Furthermore, the coherent elastic energy produced in isothermal ω transition is much larger than that caused by athermal ω transition duo to the lattice misfit between ω_{iso} and β being greater than the misfit between ω_{ath} and β. In addition, the coherent elastic energy caused by ω precipitation is found to be an increasing function of $|v_F - v_S|$ for the two kinds of transitions.

References

1. Nag S, Banerjee R, Srinivasan R, Hwang JY, Harper M, Fraser HL (2009) Acta Mater 57:2136
2. Prima F, Vermaut P, Texier G, Ansel D, Gloriant T (2006) Scripta Mater 54:645
3. Ohmori Y, Ogo T, Nakai K, Kobayashi S (2001) Mater Sci Eng A 312:182
4. Banerjee S, Mukhopadhyay P (2007) Phase transformations: examples from titanium and zirconium alloys. Elsevier, Oxford
5. Banerjee S, Dey GK (2004) J Mater Sci 39:3985. doi: 10.1023/B:JMSC.0000031480.14624.a4
6. Cook HE (1975) Acta Met 23:1041
7. Farjami S, Kubo H (2005) Acta Mater 53:1693
8. Khachaturyan AG (1983) Theory of structural transformation in solids. Wiley, New York
9. Wang Y, Khachaturyan AG (1997) Acta Mater 45:759
10. Aurelio G, Fernandez Guillermet A, Cuello GJ, Campo J (2005) J Nucl Mater 341:1
11. Aurelio G, Guillermet AF, Cuello GJ, Campo J (2003) Mater Trans A 34A:2771
12. Aurelio G, Fernandez Guillermet A, Cuello GJ, Campo J (2002) J Alloys Comp 335:132
13. Aurelio G, Guillermet A, Cuello G, Campo J (2001) Metall Mater Trans A 32:1903
14. Toda Y, Nakagawa H, Koyama T, Miyazaki T (1998) Mater Sci Eng A 255:90
15. Grad G, Fernandez GA, Rolando GJ (1996) Z Metallkd 87:726
16. Sass SL, Borie B (1972) J Appl Cryst 5:236
17. Shen C, Simmons JP, Wang Y (2006) Acta Mater 54:5617
18. Shen C, Simmons JP, Wang Y (2007) Acta Mater 55:1457
19. Hickman BS (1969) J Mater Sci 4:554. doi:10.1007/BF00550217